www.sciencetranslationalmedicine.org/cgi/content/full/4/141/141ra90/DC1

Supplementary Materials for

Pharmacological Rescue of Mitochondrial Deficits in iPSC-Derived Neural Cells from Patients with Familial Parkinson's Disease

Oliver Cooper, Hyemyung Seo, Shaida Andrabi, Cristina Guardia-Laguarta, John Graziotto, Maria Sundberg, Jesse R. McLean, Luis Carrillo-Reid, Zhong Xie, Teresia Osborn, Gunnar Hargus, Michela Deleidi, Tristan Lawson, Helle Bogetofte, Eduardo Perez-Torres, Lorraine Clark, Carol Moskowitz, Joseph Mazzulli, Li Chen, Laura Volpicelli-Daley, Norma Romero, Houbo Jiang, Ryan J. Uitti, Zhigao Huang, Grzegorz Opala, Leslie A. Scarffe, Valina L. Dawson, Christine Klein, Jian Feng, Owen A. Ross, John Q. Trojanowski, Virginia M.-Y. Lee, Karen Marder, D. James Surmeier, Zbigniew K. Wszolek, Serge Przedborski, Dimitri Krainc, Ted M. Dawson, Ole Isacson*

*To whom correspondence should be addressed. E-mail: isacson@hms.harvard.edu

Published 4 July 2012, *Sci. Transl. Med.* **4**, 141ra90 (2012)
DOI: 10.1126/scitranslmed.3003985

The PDF file includes:

Table S4. Healthy subjects' and PD patients' specific neural cell sensitivity to low concentrations of chemical stressors (mean ± SEM of % change in cell counts from vehicle-administered cultures).

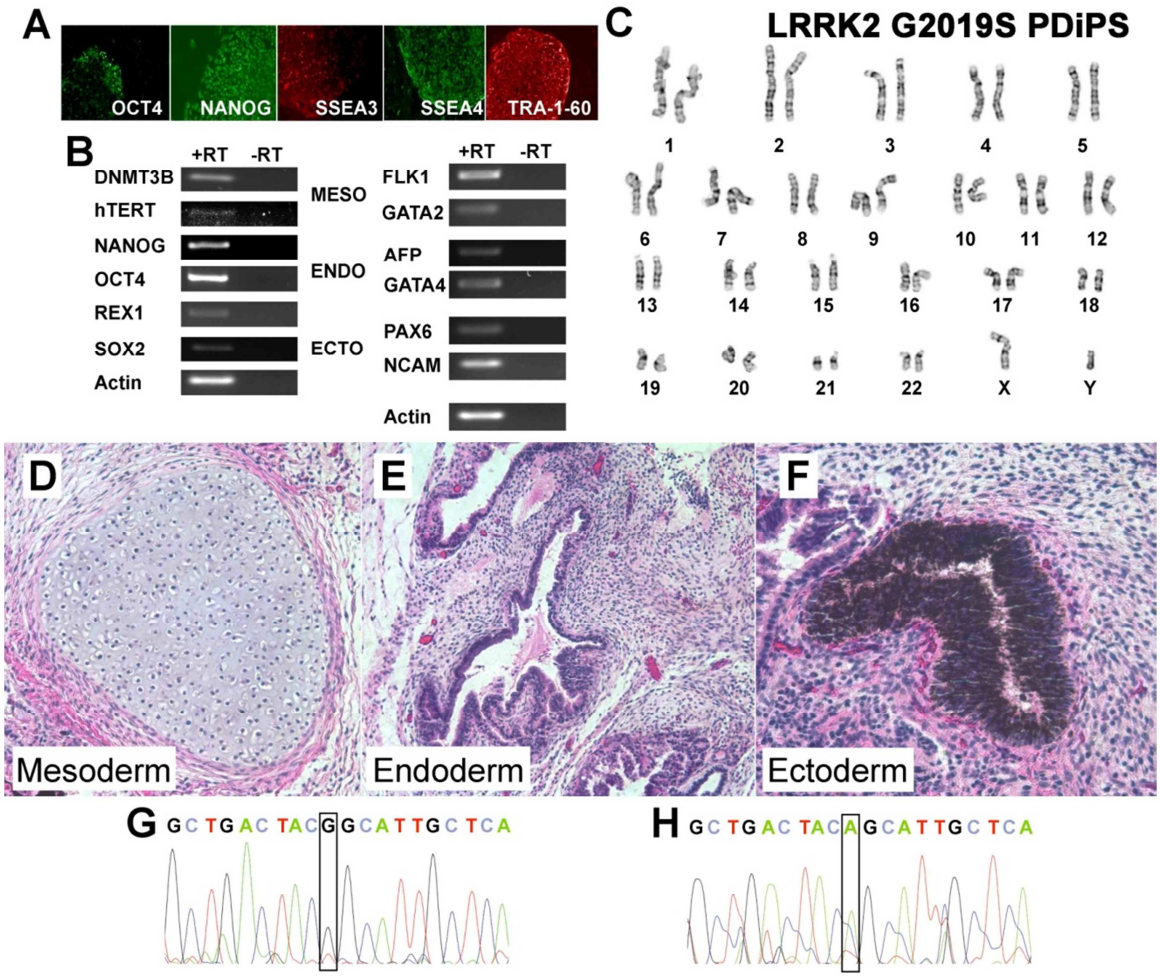

Fig. S1. Cellular reprogramming of fibroblasts from a PD patient with a homozygous *LRRK2* G2019S mutation. **(A)** Immunocytochemistry demonstrated that *LRRK2* G2019S PDiPS cells expressed pluripotency markers. **(B)** RT-PCR revealed that *LRRK2* G2019S PDiPS cells expressed further pluripotency-associated genes. Upon differentiation into embryoid bodies, RT-PCR detected the expression of mesoderm, ectoderm and endoderm-associated genes. **(C)** G-banding of metaphase *LRRK2* PDiPS cells confirmed a normal male karyotype. **(D-F)** Haematoxylin and eosin stained sections of teratomas showing iPS cell differentiation into cartilage (D, mesoderm), glandular structures (E, endoderm) and pigmented epithelium (F, ectoderm). **(G & H)** Representative chromatogram of human *LRRK2* exon 31 genomic DNA from human ES cells **(G)** and homozygous *LRRK2* G2019S iPS cells **(H)**.

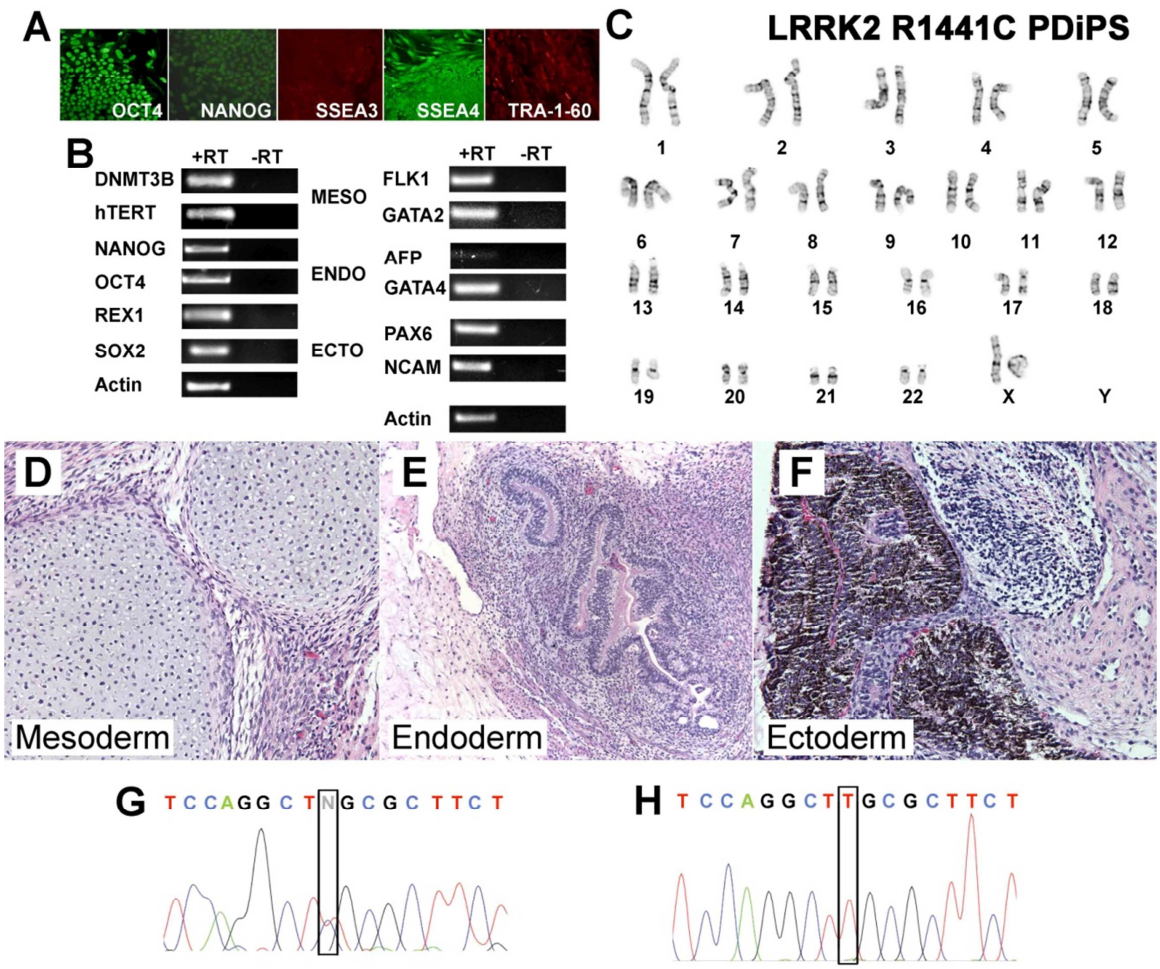

Fig. S2. Cellular reprogramming of fibroblasts from a PD patient with a heterozygous *LRRK2* R1441C mutation. **(A)** Immunocytochemistry demonstrated that *LRRK2* R1441C PDiPS cells expressed pluripotency markers. **(B)** RT-PCR revealed that *LRRK2* R1441C PDiPS cells expressed further pluripotency-associated genes. Upon differentiation into embryoid bodies, RT-PCR detected the expression of mesoderm, ectoderm and endoderm-associated genes. **(C)** G-banding of metaphase *LRRK2* R1441C PDiPS cells confirmed a normal female karyotype. **(D-F)** Haematoxylin and eosin stained sections of teratomas showing iPS cell differentiation into cartilage (D, mesoderm), glandular structures (E, endoderm) and pigmented epithelium (F, ectoderm). **(G)** A representative chromatogram of directly sequenced human *LRRK2* exon 31 genomic DNA showing heterozygosity in *LRRK2* R1441C iPS cells. Parallel direct sequencing of the same genomic region in human ES cells identified a cytosine at this position (no mutation). **(H)** To confirm the mutation, PCR products of human *LRRK2* exon 31 genomic DNA from heterozygous *LRRK2* R1441C iPS cells were sequenced. The chromatogram indicates a C>T mutation and the mutation ratio of the sequenced clones was consistent with a heterozygous *LRRK2* R1441C genomic mutation.

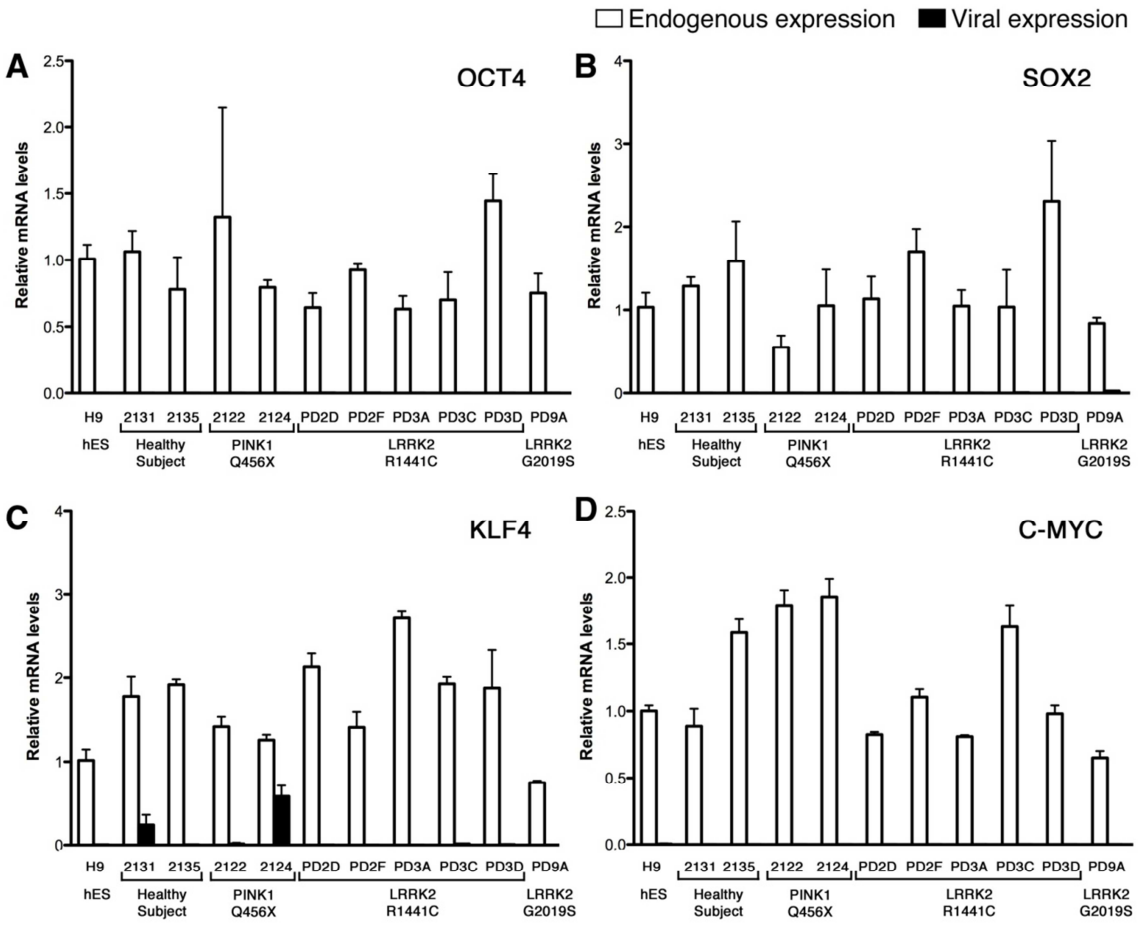

Fig. S3. Transgene silencing in iPSC lines. Quantitative PCR for endogenous (white bars) and transgene-specific (black bars) transcripts for OCT4, KLF4, SOX2 and C-MYC expressed relative to human ES cell levels ($2^{-\Delta\Delta_{CT}}$).

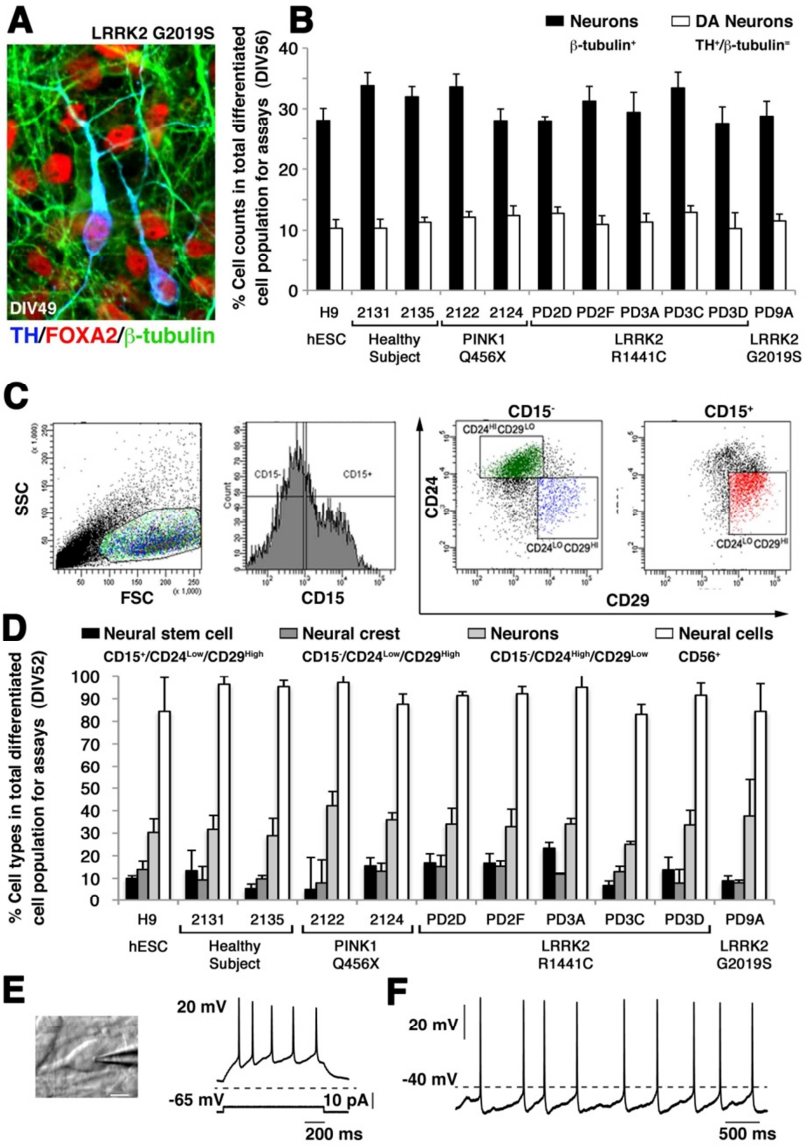

Fig. S4. Categories of cell types differentiated from iPSC lines used in phenotypic assays. (A) Immunocytochemistry of cultures differentiated from *LRRK2* G2019S PDiPS revealed ventral midbrain type dopaminergic neurons that characteristically coexpressed TH (blue), FOXA2 (red) and β-tubulin (green). **(B)** Cell counts from differentiated PDiPS cells demonstrated similar yields of neurons and DA neurons from each human pluripotent stem cell line used for phenotypic assays. **(C,D)** FACS analysis of differentiated PDiPS cell lines at DIV52 showed similar populations of neural cell types, independent of genotype. (D) Representative images of gating strategies for the neural code. (E) Quantification of the neural cell populations from FACS analysis demonstrated similar yields from each human pluripotent stem cell line examined. **(E)** By DIV70, patient-specific neurons were identified by phase contrast microscopy and whole cell current clamp recording demonstrated action potentials that were elicited by current injection and **(F)** spontaneous firing.

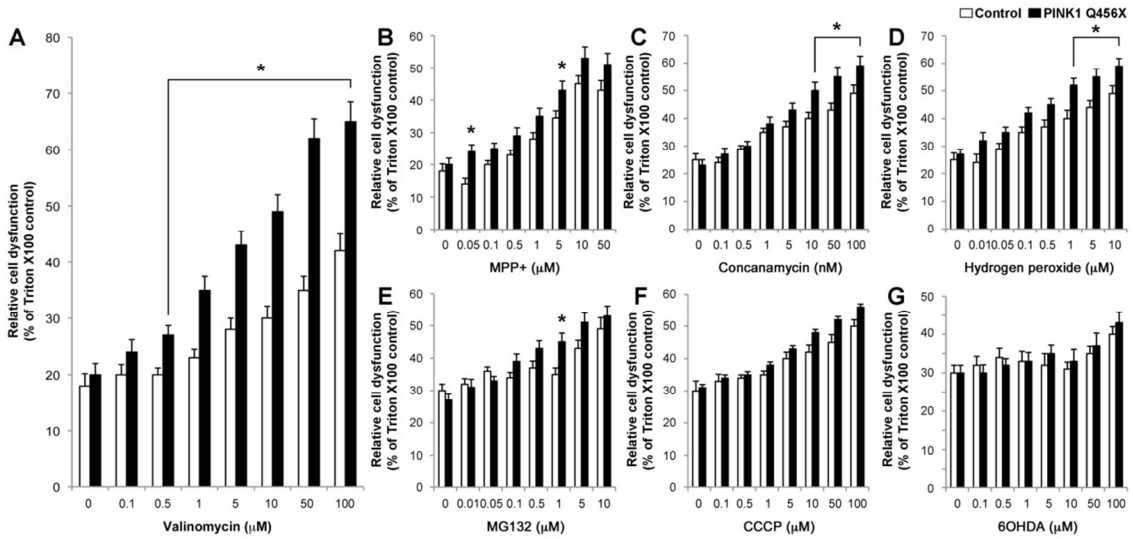

Fig. S5. The vulnerability profile of *PINK1* Q456X homozygote patient-specific neural cells. Cytotoxicity of *PINK1* patient-specific neural cells (black bars) or healthy subject neural cells (white bars) was assessed by LDH release after exposure to different concentrations of PD-associated toxins. *PINK1* patient-specific neural cells were more sensitive than healthy subject neural cells to specific concentrations of valinomycin (A), MPP+ (B), concanamycin A (C), hydrogen peroxide (D) and MG132 (E) but not CCCP (F) nor 6OHDA (G). * = ANOVA $p<0.05$.

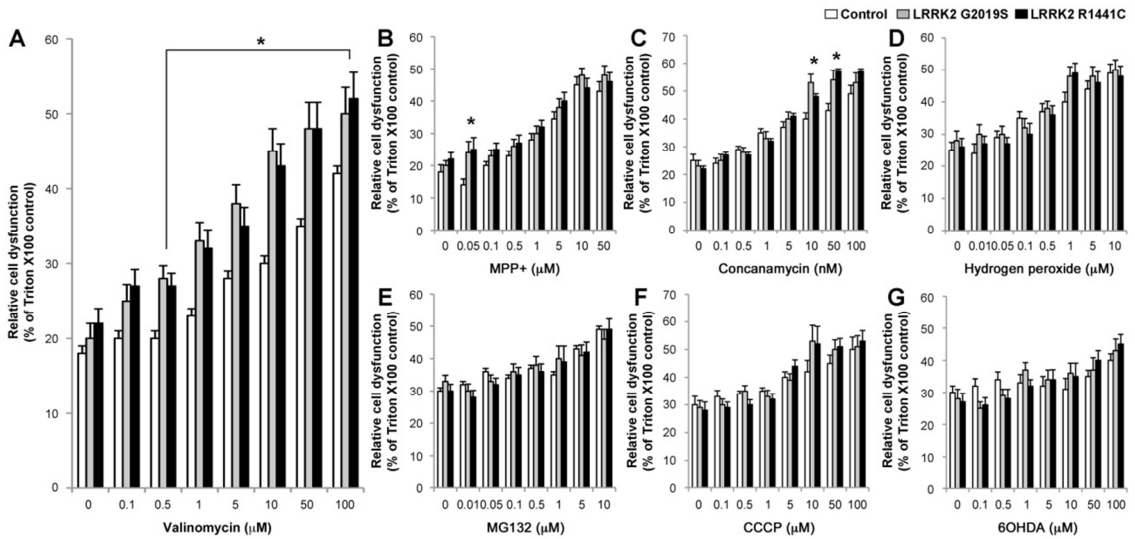

Fig. S6. The vulnerability profile of *LRRK2* patient-specific neural cells. Cytotoxicity of *LRRK2* G2019S (grey bars) and R1441C (black bars) patient-specific neural cells or healthy subject neural cells (white bars) was assessed by measuring LDH release after exposure to different concentrations of PD-associated toxins. Both *LRRK2* G2019S and R1441C patient-specific neural cells were more sensitive than healthy subject neural cells to specific concentrations of valinomycin (A), MPP+ (B), concanamycin A (C) but not hydrogen peroxide (D), MG132 (E), CCCP (F) nor 6OHDA (G). * = ANOVA $p<0.05$.

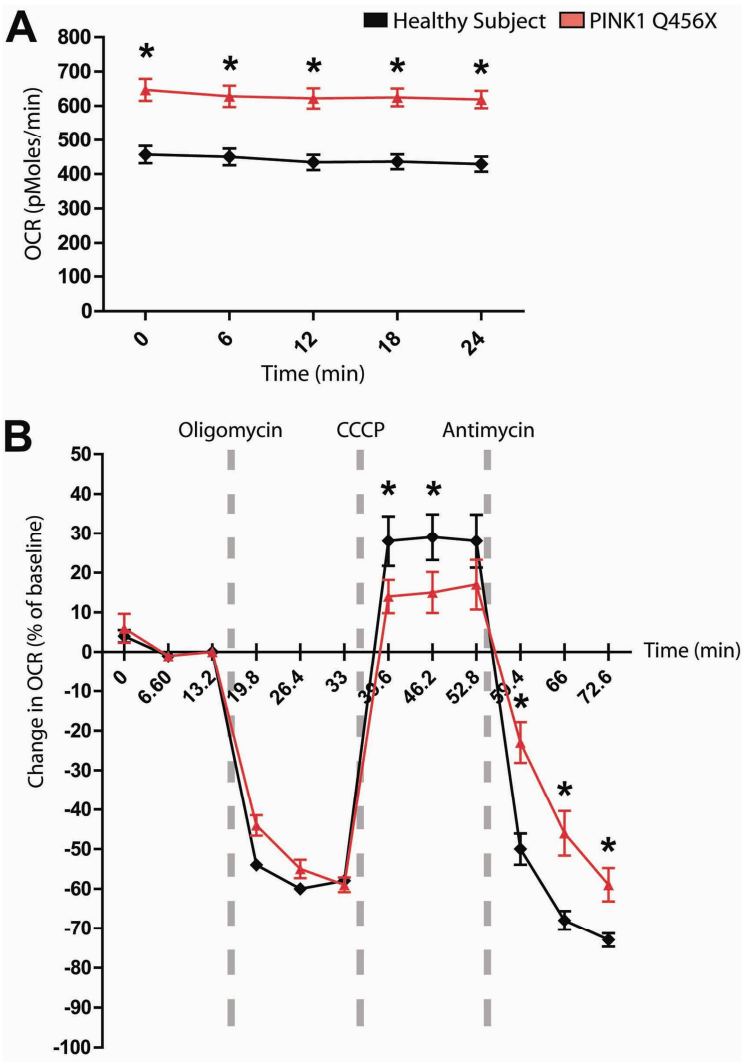

Fig. S7. Increased basal respiration and oxygen consumption of *PINK1* patient neural cells. (A) Baseline oxygen consumption rates (OCR) were measured in Healthy subject (black) and PINK1 Q456X (red) neural cells using the Seahorse extracellular flux analyzer over a period of 24 minutes. The baseline OCR of PINK1 neural cells was significantly higher than neural cells from healthy subjects. (B) Healthy subject and PINK1 cells were administered oligomycin, CCCP, and Antimycin A sequentially and the OCR was plotted relative to baseline conditions. Following CCCP treatment, PINK1 neural cells exhibited a decreased reserve capacity (~15%) compared to healthy subject neural cells (~29%), indicating that at baseline, PINK1 mitochondria are at a heightened state of oxygen consumption than the healthy subject control mitochondria.

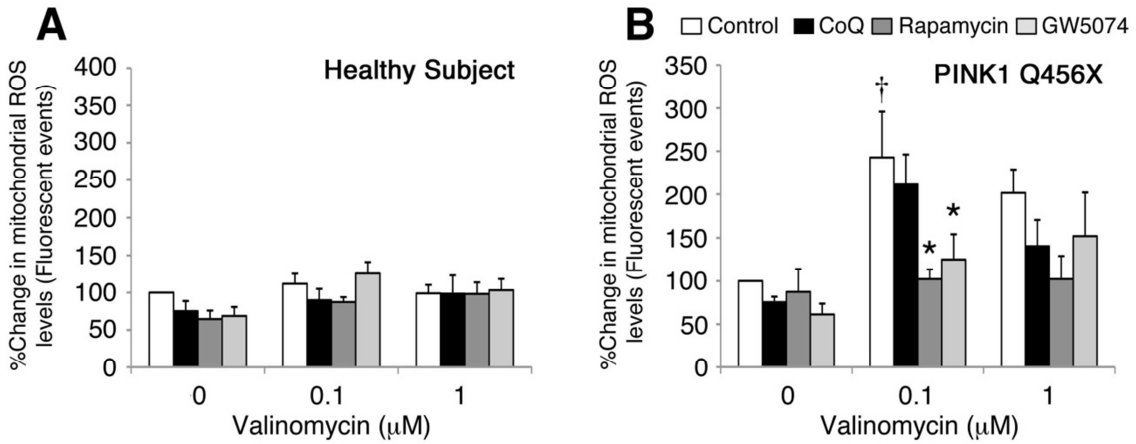

Fig. S8. Treatment with rapamycin or GW5074 reduces mROS levels in *PINK1* patient neural cells caused by a low dose of valinomycin. (A) Treatment of healthy subject neural cells with 1 μM Coenzyme Q_{10} (black bars), 1 μM rapamycin (dark grey bars) or 1 μM GW5074 (light grey bars) did not change mROS levels with or without exposure to valinomycin. **(B)** Exposure to 0.1 μM valinomycin increased mROS levels in *PINK1* patient neural cells (white bars). Treatment with either rapamycin or GW5074 reduced mROS levels in *PINK1* patient neural cells induced by 0.1 μM valinomycin. Data are represented as Mean ± SEM. * $p<0.05$ ANOVA versus valinomycin administered control *PINK1* patient neural cells, † $p<0.05$ ANOVA versus control *PINK1* patient neural cells not exposed to valinomycin.

Table S1. Patient genotypes and cellular reprogramming methods.

Subject ID	Line/Clone ID	Genotype	Retrovirus Method
1	2122	*PINK1* Q456X Homo	OCT4, KLF4, SOX2, C-MYC (*27*)
2	2124	*PINK1* Q456X Homo	OCT4, KLF4, SOX2, C-MYC (*27*)
3	PD2D	*LRRK2* R1441C	OCT4, KLF4, SOX2, C-MYC/VPA (*63*)
3	PD2F	*LRRK2* R1441C	OCT4, KLF4, SOX2, C-MYC/VPA (*63*)
4	PD3A	*LRRK2* R1441C	OCT4, KLF4, SOX2, C-MYC/VPA (*63*)
4	PD3C	*LRRK2* R1441C	OCT4, KLF4, SOX2, C-MYC/VPA (*63*)
4	PD3D	*LRRK2* R1441C	OCT4, KLF4, SOX2, C-MYC/VPA (*63*)
5	PD9A	*LRRK2* G2019S Homo	OCT4, KLF4, SOX2, C-MYC/VPA (*63*)
6	2131	None detected	OCT4, KLF4, SOX2, C-MYC (*27*)
7	2135	None detected	OCT4, KLF4, SOX2, C-MYC (*27*)

Table S2. PCR primer sequences (5′-3′).

Target	Forward Primer	Reverse Primer
LRRK2 Intron 30-31	tcaacaggaatgtgagcagg	cccacaattttaagtgagttgc
LRRK2 Intron 40-Exon 41	gagcacagaatttttgatgcttg	ttttatccccattccacagcagtac
PINK1 Exon 7	gagttcagattagcccatgg	gaccttcactctggaacgag
HBB Exon 2	ttggacccagaggttctttg	gagccaggccatcactaaag
B2M Exon 2	ctcacgtcatccagcagaga	agtgggggtgaattcagtgt
Actin	ggacttcgagcaagagatgg	agcactgtgttggcgtacag
DNMT3b	ataagtcgaaggtgcgtcgt	ggcaacatctgaagccattt
TERT	tgtgcaccaacatctacaag	gcgttcttggctttcaggat
NANOG	tccaacatcctgaacctcag	cgctgattaggctccaacca
OCT4 (endogenous)	gtggaggaagctgacaacaa	caggttttctttccctagct
REXI	tggacacgtctgtgctcttc	gtcttggcgtcttctcgaac
SOX2 (endogenous)	agctacagcatgatgcagga	ggtcatggagttgtactgca
AFP	agcttggtggtggatgaaac	ccctcttcagcaaagcagac
FLK1	agtgatcggaaatgacactgga	gcacaaagtgacacgttgagat
GATA2	gcaacccctactatgccaacc	cagtggcgtcttggagaag
NCAM	atggaaactctattaaagtgaacctg	tagacctcatactcagcattccagt

PAX6	tctaatcgaagggccaaatg	tgtgagggctgtgtctgttc
OCT4 (endogenous)	atgcacaacgagaggattttga	ctttgtgttcccaattccttcc
KLF4 (endogenous)	cccaattacccatccttcct	acgatcgtcttcccctcttt
SOX2 (endogenous)	cactgcccctctcacacatg	tcccatttccctcgtttttct
C-MYC (endogenous)	agcagaggagcaaaagctcatt	ccaaagtccaatttgaggcagt
WRE (for transgene)		caaattttgtaatccagaggttga

Table S3. Healthy subjects' and PD patients' specific neural cell mROS levels in response to chemical stressors (nean ± SEM of % change in mitochondrial ROS levels).

Cellular stressor / Neural cell genotype	MPP+ (μM)		Concanamycin A (nM)		MG132 (μM)		CCCP (μM)		6OHDA (μM)	
	0.5	5	1	10	1	10	1	10	1	10
Healthy subjects	125.1 ± 14.29	123.88 ± 10.98	101.42 ± 8.79	123.23 ± 15.98	107.27 ± 3.66	107.61 ± 7.1	111.75 ± 26.94	129.21 ± 34.02	88.92 ± 5.17	96.76 ± 19.07
PINK1 Q456X homozygotes	103.98 ± 8.11	100.98 ± 5.01	114.55 ± 9.3	137.32 ± 20.63	110.6 ± 17.49	138.78 ± 8.85	92.49 ± 6.88	117.65 ± 12.29	69.73 ± 12.84	83.58 ± 5.89
LRRK2 G2019S homozygote	105.83 ± 27.21	101.08 ± 27.21	149.16 ± 60.79	146.49 ± 47.01	123.7 ± 10.23	97.24 ± 11.4	91.48 ± 2.94	103.02 ± 12.26	114.87 ± 17.02	93.47 ± 8.8
LRRK2 R1441C heterozygotes	108.89 ± 6.13	122.71 ± 13.13	104.52 ± 9.57	128.16 ± 9.94	115.76 ± 12.43	113.12 ± 12.43	124.12 ± 9.65	143.22 ± 13.66	112.1 ± 5.39	114.94 ± 11.54

Table S4. Healthy subjects' and PD patients' specific neural cell sensitivity to low concentrations of chemical stressors (mean ± SEM of % change in cell counts from vehicle-administered cultures). ***** p<0.05 ANOVA versus healthy subject neural cells, **†** p<0.05 ANOVA versus untreated neural cells from same iPS cell line.

Neural cell genotype \ Cellular stressor		Valinomycin		MPP+		Concanamycin A		Hydrogen peroxide		MG132		CCCP		6OHDA	
		0.1 μM	1 μM	0.5 μM	5 μM	1 nM	10 nM	1 μM	10 μM	1 μM	10 μM	1 μM	10 μM	0.1 μM	1 μM
Healthy subjects	Total neural cells	92.3 ± 6.1	103.5 ± 10.1	89.0 ± 9.5	97.9 ± 15.9	96.1 ± 3.1	100.6 ± 3.1	93.8 ± 6.7	103.7 ± 24.8	107.6 ± 8.49	109.6 ± 24.8	102.7 ± 12.8	104.9 ± 12.7	111.8 ± 5.8	127.5 ± 7.2
	Neurons	86.8 ± 5.9	106.8 ± 5.6	96.0 ± 15.9	103.5 ± 7.6	111.3 ± 3.7	109.2 ± 4.8	114.2 ± 7.8	89.2 ± 10.1	100.3 ± 8.5	91.7 ± 7.2	106.2 ± 14.4	91.6 ± 13.9	119.9 ± 11.0	111.4 ± 21.0
	DA neurons	99.7 ± 9.0	96.0 ± 12.3	96.3 ± 9.0	92.3 ± 7.5	109.7 ± 8.3	98.6 ± 7.0	87.1 ± 10.9	120.7 ± 18.4	122.2 ± 20.8	88.3 ± 6.4	103.4 ±12.1	109.5 ± 9.0	111.2 ± 21.0	122.0 ± 18.1
PINK1 Q456X homo.	Total neural cells	95.5 ± 4.9	79.9 ± 9.4	114.1 ± 11.1	99.6 ± 4.8	95.4 ± 7.4	96.2 ± 4.3	84.4 ± 10.4	80.3 ± 13.6	101.3 ± 2.4	76.7 ± 10.1	87.8 ± 8.6	90.3 ± 5.7	101.7 ± 6.1	110.8 ± 3.9
	Neurons	82.4 ± 4.9	76.7 ± 9.4***†**	115.4 ± 18.7	108.2 ± 22.1	84.7 ± 12.0	79.7 ± 12.6	97.8 ± 5.3	120.6 ± 13.2	107.7 ± 17.5	103.9 ± 19.5	121.2 ± 9.7	79.8 ± 5.7	99.3 ±9.3	110.3 ± 9.5
	DA neurons	82.8 ± 7.6	65.8 ± 10.5**†**	116.55 ± 5.5	99.9 ± 3.9	92.4 ± 8.9*****	84.0 ± 4.6	113.7 ± 7.6	89.4 ± 24.1	119.6 ± 5.2	116.3 ± 19.3	107.4 ± 6.4	92.3 ± 8.8	101.6 ± 1.3	106.2 ± 7.3
LRRK2 G2019S homo	Total neural cells	100 ± 4.1	83.7 ± 12.4	100.9 ± 5.9	93.7 ± 8.5	96.3 ± 3.8	91.4 ± 4.9	114.3 ± 9.9	110.2 ± 15.9	114.3 ± 9.9	110.2 ± 15.9	93.5 ± 6.3	97.6 ± 2.7	99.2 ± 12.7	114.9 ± 4.8
	Neurons	93.0 ± 7.5	100.4 ± 16.5	124.5 ± 25.1	92.2 ± 20.7	94.5 ± 10.8	89.6 ± 4.9	95.1 ± 9.9	62.9 ± 6.0	96.6 ± 11.8	62.9 ± 6.0	81.9 ± 13.7	117.7 ± 6.0	95.3 ± 13.9	88.1 ± 9.7
	DA neurons	83.5 ± 19.1	89.7 ± 10.1	131.8 ± 23.2	111.2 ± 12.6	109.9 ± 7.7	104.4 ± 6.7	92.2 ± 3.0	81.7 ± 5.5	92.2 ± 3.0	81.7 ± 5.5	116.6 ± 5.9	112.9 ± 15.1	105.5 ± 2.5	100.5 ± 4.2
LRRK2 R1441C het.	Total neural cells	73.8 ± 5.4	71.3 ± 4.8***†**	102.3 ± 4.4	100.3 ± 9.0	89.2 ± 4.2	86.6 ± 4.3**†**	79.36 ± 8.1	75.9 ± 15.9	101.9 ± 10.0	96.4 ± 9.1	82.6 ± 6.6	88.2 ± 8.1	94.3 ± 4.2*****	85.2 ± 4.3*****
	Neurons	78.5 ± 6.8**†**	76.9 ± 4.8***†**	90.3 ± 5.7	84.2 ± 9.9	95.2 ± 3.8*****	90.5 ± 4.1*****	95.1 ± 9.9	102.1 ± 8.9	98.4 ±16.2	93.5 ± 17.5	103.1 ± 11.8	93.2 ± 8.1	77.0 ± 3.8	61.8 ± 4.1
	DA neurons	66.0 ± 4.0***†**	60.9 ± 4.6***†**	104.2 ± 8.5	88.4 ± 9.7	93.6 ± 6.3*****	80.1 ± 3.7*****	86.32 ± 8.6	100.2 ±13.3	101.7 ± 5.6	96.8 ± 15.9	94.2 ± 11.8	90.1 ± 5.5	78.5 ± 6.3	64.5 ± 3.7*****